Experimental Analysis of Correlations in the Nonlinear Phase Noise in Optical Fiber Systems

Tobias Fehenberger[1], Mikael Mazur[2], Tobias A. Eriksson[3], Magnus Karlsson[2], and Norbert Hanik[1]

[1] Institute for Communications Engineering, Technical University of Munich (TUM), Munich, Germany
[2] Dept. of Microtechnology and Nanoscience, Chalmers University of Technology, Gothenburg, Sweden
[3] Nokia Bell Labs, Lorenzstr. 10, 70435 Stuttgart, Germany
tobias.fehenberger@tum.de

Abstract *A dual-link self-homodyne receiver is used to measure the phase correlations introduced by the interplay of dispersion and fiber nonlinearities. The dependence of the memory on the WDM setup, signal power and transmission distance is experimentally demonstrated.*

Introduction

While the demand for increased throughput of fiber-optic systems is continuously growing, their maximum data rates are to-date limited by nonlinear interactions between co-propagating channels, and within the channel of interest. This limitation has resulted in detailed studies of constraints induced by fiber nonlinearities[1].

Popular capacity lower bounds[2] included the compensation for intra-channel distortions, but treated the nonlinear interference (NLI) of the wavelength-division multiplexing (WDM) neighbors as noise that cannot be compensated in a network setup. Recent studies of point-to-point links show that the nonlinear phase noise (NLPN) is correlated over time[3,4]. This memory can be exploited, e.g., by using an equalizer[5] or with carrier phase estimation (CPE) techniques[6], and NLPN can be reduced. A study of the correlation properties, however, is impeded by laser phase noise (LPN) present in practical systems[7].

Most coherent optical communication systems use intradyne detection where a free-running local oscillator (LO) laser beats with the signal. The LPN of transmit and LO laser is then removed by CPE in the digital signal processing (DSP) unit. In such a system, NLPN and LPN mix and cannot be distinguished[7]. Therefore, the properties of NLPN can only be studied indirectly in intradyne detection experiments with LPN, and recent results[8,9] show that the NLPN can be mitigated by optimizing the CPE length. It is, however, impossible to directly measure the auto-correlation function (ACF) of the NLPN as it depends on the CPE length[7].

In this paper, we bypass this limitation by using a self-homodyne (SH) setup in which the laser pilot tone is transmitted over a second fiber, enabling measurements without nonlinear interactions of the pilot and the signal. Without CPE and frequency offset estimation in the DSP, the dependence of the NLPN correlations on launch power, WDM spacing and transmission distance is experimentally verified. To the best of our knowledge, this is the first direct experimental observation of correlations introduced by fiber nonlinearities using a SH receiver.

Theoretical Background

The optical channel is modeled by a partially coherent AWGN channel for which the distortions are split into additive and phase noise terms,

$$\boldsymbol{y}_k = \boldsymbol{x}_k \cdot e^{j\boldsymbol{\phi}_k} + \boldsymbol{n}_k^{\mathrm{NLI}} + \boldsymbol{n}_k^{\mathrm{ASE}}, \tag{1}$$

where $\boldsymbol{x}$ is the channel input, $\boldsymbol{y}$ the recovered sequence after DSP, and k indices time instant of a sequence of length N. We treat both $\boldsymbol{n}_k^{\mathrm{ASE}}$ and $\boldsymbol{n}_k^{\mathrm{NLI}}$ as uncorrelated over time[4]. While this assumption is true for ASE noise, it is a simplifying approximation for the additive NLI. The NLPN $\boldsymbol{\phi}_k$ is correlated over time due to intra-channel and inter-channel nonlinearities.

We extract the radial difference $\boldsymbol{\theta}_k$ between $\boldsymbol{y}_k$ and $\boldsymbol{x}_k$ as

$$\boldsymbol{\theta}_k = \frac{\boldsymbol{x}_k^* \boldsymbol{y}_k}{|\boldsymbol{x}_k^* \boldsymbol{y}_k|}, \tag{2}$$

where $(\cdot)^*$ denotes complex conjugate and the normalization is done to remove the multiple amplitude levels of $\boldsymbol{x}$. As (2) effectively removes the modulation from $\boldsymbol{y}_k$, $\boldsymbol{\theta}_k$ captures uncorrelated noise contributions from the complex additive noise terms $\boldsymbol{n}_k^{\mathrm{ASE}}$ and $\boldsymbol{n}_k^{\mathrm{NLI}}$ as well as correlated NLI. To be able extract the phase correlations within the dominant uncorrelated noise in $\boldsymbol{\theta}_k$, we take a moving average over $w+1$ symbols and the $\arg$ to extract the angle,

$$\bar{\boldsymbol{\theta}}_k = \arg\Big(\sum_{l=-w/2}^{w/2} \boldsymbol{\theta}_{k+l} \Big). \tag{3}$$

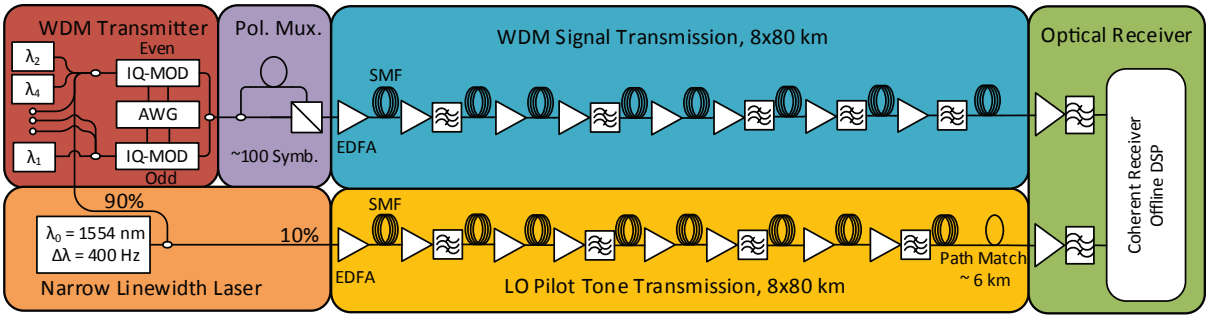

Fig. 1: Experimental setup of the dual-link self-homodyne system. The upper part shows the signal transmission line while the lower branch presents the line for the LO. The links are matched in length to ensure that the two signals do not lose correlation.

The ACF $R_{\bar{\theta}}[\tau]$ of $\bar{\boldsymbol{\theta}}$ at delay τ is

$$R_{\bar{\theta}}[\tau] = \frac{\mathrm{E}\{\bar{\boldsymbol{\theta}}_k \bar{\boldsymbol{\theta}}_{k-\tau}\}}{N-\tau} = \frac{\mathcal{F}^{-1}\{|\mathcal{F}\{\bar{\boldsymbol{\theta}}_k\}|^2\}}{N-\tau}, \quad (4)$$

where $\mathrm{E}\{\cdot\}$ denotes expectation, $\mathcal{F}\{\cdot\}$ is Fourier transform, and dividing by $N-\tau$ gives an unbiased estimate. Note that the ACF $R_{\bar{\theta}}[\tau]$ will not resemble a Dirac delta function even in the absence of correlations because the averaging in (3) introduces correlations over w symbols. Thus, the ACF for uncorrelated $\boldsymbol{\theta}$'s will linearly decline from its peak $R_{\bar{\theta}}[0]$ to $R_{\bar{\theta}}[w] = 0$. If the ACF deviates from this shape, temporal correlations in the phase are observed. Further note that $R_{\bar{\theta}}[0]$ is the variance of $\bar{\boldsymbol{\theta}}$ and thus describes the correlation strength between adjacent symbols.

Experimental Setup

The experimental setup is outlined in Fig. 1 and consists of two separate straight line links to transmit the signal and the LO separately. We use a narrow linewidth laser (400 Hz) for the central carrier and an additional set of <100 kHz linewidth lasers to generate WDM loading carriers. The lasers are separated into even and odd carriers and modulated using two separate IQ modulators. The modulators are driven by an arbitrary waveform generator (AWG) generating a 20 GBaud 16QAM signal using 4 digital-to-analog converters operating at 60 GS/s. A root-raised cosine filter with a roll-off of 0.05 was used. The data on even and odd carriers was decorrelated by ~1000 symbols.

All carriers are combined before a polarization-multiplexing emulation stage. The launch power per channel is always −2.5 dBm unless otherwise stated. The signal is transmitted over 8 spans, each consisting of 80 km standard single mode fiber (SMF) and an Erbium-doped fiber amplifier (EDFA) to compensate for the loss. Wave shapers and bandpass filters are inserted for gain equalization and to suppress out-of-band noise, respectively.

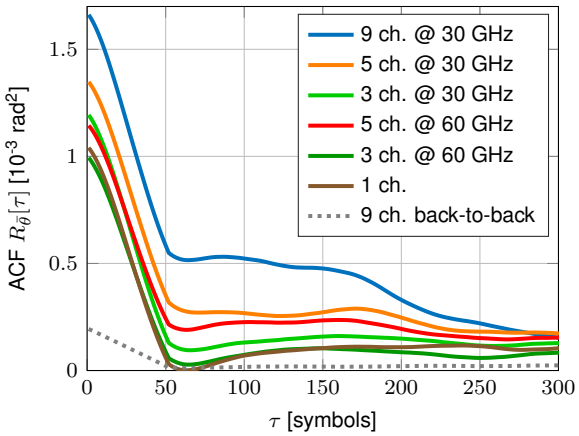

Fig. 2: ACF for varying number of WDM channels (and thus total power) and WDM spacings over 640 km (solid), with $w = 51$. Back-to-back results (dotted) show no correlations.

A similar link is used to transmit a portion of the central laser that is used as LO at the receiver. This link separation ensures that no nonlinear interference between signal and LO occurs during propagation. The length difference of the two links was less than 100 m after the path-matched fiber was inserted. The signals are detected using a conventional coherent receiver and sampled using a 50 GS/s real-time oscillsocope. Offline DSP with equalization and polarization demultiplexing based on decision-directed least mean square with the constant modulus algorithm for pre-convergence is applied. No CPE or frequency estimation was used.

Results

In Fig. 2, the ACF for different WDM setups is shown. Only the x-polarization is presented because all results of the two polarizations are in full agreement. The strongest NLI for all considered WDM setups is observed for 9 WDM channels with an ACF peak at 1.7×10^{-3} rad^2. We further observe that the amount of memory increases with the number of co-propagating channels. Since the fiber setup and the receiver DSP have remained identical, we argue that the ACF for 9 channels over 640 km shows temporal cor-

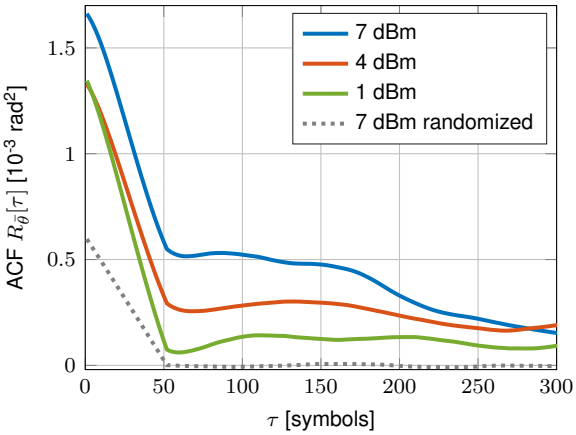

Fig. 3: ACF for 9 WDM channels over 640 km at total powers of 1 dBm, 4 dBm, and 7 dBm, with $w = 51$. The ACF of randomized symbols (dotted) shows no temporal correlations.

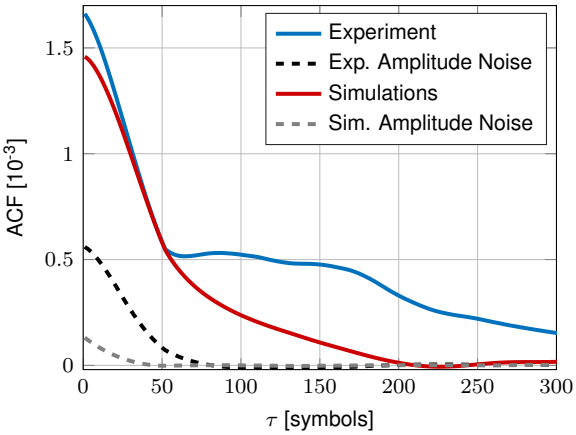

Fig. 4: ACF $R_{\bar{\theta}}[\tau]$ for phase noise (solid) and ACF for amplitude noise (dashed) in experiments and simulations with 9 channels spaced at 30 GHz, 7 dBm total power, and w=51.

relations from the interplay of dispersive memory and inter-channel nonlinear crosstalk. No significant memory is observed for 1 and 3 WDM channels because the total power is too low. Note that the fluctuations at larger delays and the saturation above zero are attributed to the non-ideal beating of the signal with the laser pilot.

The impact of varying the total signal power is investigated for 9 WDM channels in Fig. 3. The temporal correlations are found to increase with signal power. Although the ACF of the NLPN does not depend on the launch power in theory, the NLPN variance depends on the quadratic launch power[4]. Therefore, a difference in correlations is seen in Fig. 3 for high powers because the phase noise is more pronounced within the otherwise uncorrelated noise. Further shown as gray dotted curve is the ACF for randomly shuffled input-output pairs $(\boldsymbol{x}_k, \boldsymbol{y}_k)$. No memory is observed, which is expected because a random permutation removes all inter-symbol correlations. This shows that there are no persistent effects in our setup that introduce correlations.

Figure 4 shows a comparison between split-step simulations and experiments for 9 channels, 640 km and 7 dBm total power. The simulations predict a steeper decay of the ACF than what is measured in the SH experiments. We observe that both experiments and simulations have a similar slope until $\tau = w = 51$ symbols, suggesting that at this point, the same amount of memory is left. For larger delays, we speculate that phase drifts of the reference laser and differences in the dual-link setup introduce further correlations in the experiments. A detailed study of this effect is part of our ongoing work, especially since the presented simulations assumed ideal lasers at transmitter and receiver and thus may not reflect the imperfections of a SH setup. For example, the measurements were sensitive to vibrations and other external influences as the setup acted as one large interferometer.

Further shown in Fig. 4 is the ACF for averaged amplitude noise, i.e., using $|\boldsymbol{y}_k - \boldsymbol{x}_k|$ instead of $\boldsymbol{\theta}_k$ in (3) without the $\arg$. No correlations are seen.

Conclusions

We have experimentally studied the nonlinear memory in a multi-span transmission system. The dependence of the correlation strength and length on the WDM setup, the launch power and the transmission distance is demonstrated. Exploiting these correlations is a potential approach to increase spectral efficiencies in next-generation optical communication systems.

References

[1] P. Poggiolini, "Recent advances in non-linear fiber propagation modeling," Proc. OFC, W3I.4, 2016.

[2] R.-J. Essiambre *et al.*, "Capacity limits of optical fiber networks," JLT **28**(4), 2010.

[3] A. Mecozzi and R.-J. Essiambre, "Nonlinear shannon limit in pseudolinear coherent systems," JLT **30**(12), 2012.

[4] R. Dar *et al.*, "Properties of nonlinear noise in long, dispersion-uncompensated fiber links," Opt. Exp. **21**(22), 2013.

[5] M. Secondini and E. Forestieri, "On XPM mitigation in WDM fiber-optic systems," PTL **26**(22), 2014.

[6] M. P. Yankov *et al.*, "Low-Complexity tracking of laser and nonlinear phase noise in WDM optical fiber systems," JLT **33**(23), 2015.

[7] T. Fehenberger *et al.*, "On the impact of carrier phase estimation on phase correlations in coherent fiber transmission," Proc. TIWDC, 2015.

[8] Y. Zhao *et al.*, "Beyond 100G optical channel noise modeling for optimized soft-decision FEC performance," Proc. OFC, OW1H.3, 2012.

[9] C. Schmidt-Langhorst *et al.*, "Experimental analysis of nonlinear interference noise in heterogeneous flex-grid WDM transmission," Proc. ECOC, Tu.1.4.3, 2015.